

# Heavy-Atom-Substituted Nucleobases in Photodynamic Applications: Substitution of Sulfur with Selenium in 6-Thioguanine Induces a Remarkable Increase in the Rate of Triplet Decay in 6-Selenoguanine

Kieran M. Farrell,<sup>†,§</sup> Matthew M. Brister,<sup>†,¶</sup> Michael Pittelkow,<sup>‡</sup> Theis I. Sølling,<sup>‡</sup> and Carlos E. Crespo-Hernández<sup>\*,†,¶</sup>

<sup>†</sup>Department of Chemistry, Case Western Reserve University, 10900 Euclid Avenue, Cleveland, Ohio 44106, United States

<sup>‡</sup>Department of Chemistry, University of Copenhagen, Universitetsparken 5, DK-2100 Copenhagen, Denmark

## S Supporting Information

**ABSTRACT:** Sulfur substitution of carbonyl oxygen atoms of DNA/RNA nucleobases promotes ultrafast intersystem crossing and near-unity triplet yields that are being used for photodynamic therapy and structural-biology applications. Replacement of sulfur with selenium or tellurium should significantly red-shift the absorption spectra of the nucleobases without sacrificing the high triplet yields. Consequently, selenium/tellurium-substituted nucleobases are thought to facilitate treatment of deeper tissue carcinomas relative to the sulfur-substituted analogues, but their photodynamics are yet unexplored. In this contribution, the photochemical relaxation mechanism of 6-selenoguanine is elucidated and compared to that of the 6-thioguanine prodrug. Selenium substitution leads to a remarkable enhancement of the intersystem crossing lifetime both to and from the triplet manifold, resulting in an efficiently populated, yet short-lived triplet state. Surprisingly, the rate of triplet decay in 6-selenoguanine increases by 835-fold compared to that in 6-thioguanine. This appears to be an extreme manifestation of the classical heavy-atom effect in organic photochemistry, which challenges conventional wisdom.

In addition to optimizing DNA for its role as the genetic blueprint of life, evolution has tailored the structure of DNA nucleotides such that they efficiently dissipate energy absorbed from ultraviolet (UV) radiation.<sup>1,2</sup> Numerous theoretical and experimental investigations have demonstrated that the naturally occurring nucleobases, nucleosides, and nucleotides recover their electronic ground states within ~1 ps of excitation.<sup>1–4</sup> Ultrafast ground-state recovery has made nucleic acids robust against the solar onslaught of one of the most ubiquitous carcinogens, UV radiation.<sup>5,6</sup> Conversely, sulfur substitution of carbonyl oxygen atoms on nucleobases leads to the efficient population of long-lived, reactive triplet excited states in high yields.<sup>7–11</sup> As a result, the photochemistry of sulfur-substituted DNA/RNA nucleobases (a.k.a., thiobases) has drawn increased attention because of their use in photodynamic therapy and photo-cross-linking applications.<sup>9–19</sup>

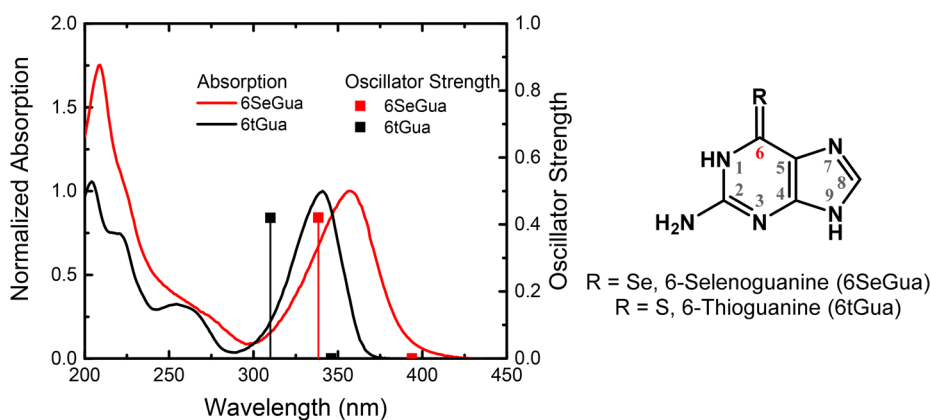
The high triplet yield makes the thiobases prime sensitizers for targeting DNA/RNA damage;<sup>10</sup> however, their absorption properties limit the applications to the treatment of skin cancer cells.<sup>12</sup> Replacement of the sulfur atom with selenium or tellurium should red-shift the absorption spectra into the visible with the potential additional benefit of maximizing their triplet yields. Recent quantum-chemical calculations predict that selenium- and tellurium-substituted nucleobases are highly promising photosensitizers.<sup>20,21</sup> By using femtosecond broadband transient absorption spectroscopy, we demonstrate that selenium substitution of guanine's carbonyl oxygen atom leads to a remarkable enhancement of the intersystem crossing (ISC) lifetime both to and from the triplet manifold. In particular, the rate of ISC to the ground state in 6-selenoguanine increases by 835-fold, or more than 2 orders of magnitude, compared to that of the 6-thioguanine (6tGua) prodrug. A strategy for harvesting the use of 6SeGua for photodynamic therapy and structural-biology applications is presented, which might enable heavy-atom-substituted nucleobases to reach their full potential.

Figure 1 shows the absorption spectra for 6SeGua and 6tGua normalized to their lowest energy  $\pi \rightarrow \pi^*$  transition. 6SeGua exhibits maxima at 357 and 209 nm, whereas 6tGua has maxima at 341, 254, and 204 nm. Selenium substitution broadens and red-shifts the UVA transition by 16 nm (1314.3  $\text{cm}^{-1}$ ) relative to sulfur substitution. The combined shifting and broadening of 6SeGua's absorption give rise to a tail absorbing in the visible region. The oscillator strength of the UVA vertical transition for 6SeGua, shown in Figure 1, has a very similar magnitude to that for 6tGua,<sup>22</sup> suggesting that the molar absorptivity in the UVA region is similar for both molecules. We estimate that using 6SeGua as photosensitizer could facilitate up to 90% deeper tissue treatment by UVA radiation than 6tGua (see Figure S1 and the Supporting Information (SI) for details).

Quantum-chemical computations have shown that the N<sup>9</sup> tautomer of 6SeGua is most stable in solution.<sup>23–26</sup> We have performed ground-state optimizations and subsequent vertical excitation energy calculations for the N<sup>9</sup> tautomer of 6SeGua

Received: July 19, 2018

Published: August 26, 2018



**Figure 1.** Ground-state absorption spectra of 6SeGua and 6tGua normalized to their lowest-energy  $\pi \rightarrow \pi^*$  transitions. All spectra were obtained in pH 7.4 phosphate buffer saline (PBS) at room temperature. Oscillator strengths obtained from TDDFT computations at the PBE0/IEF-PCM/6-311++G(d,p) level of theory are included (see SI for details).

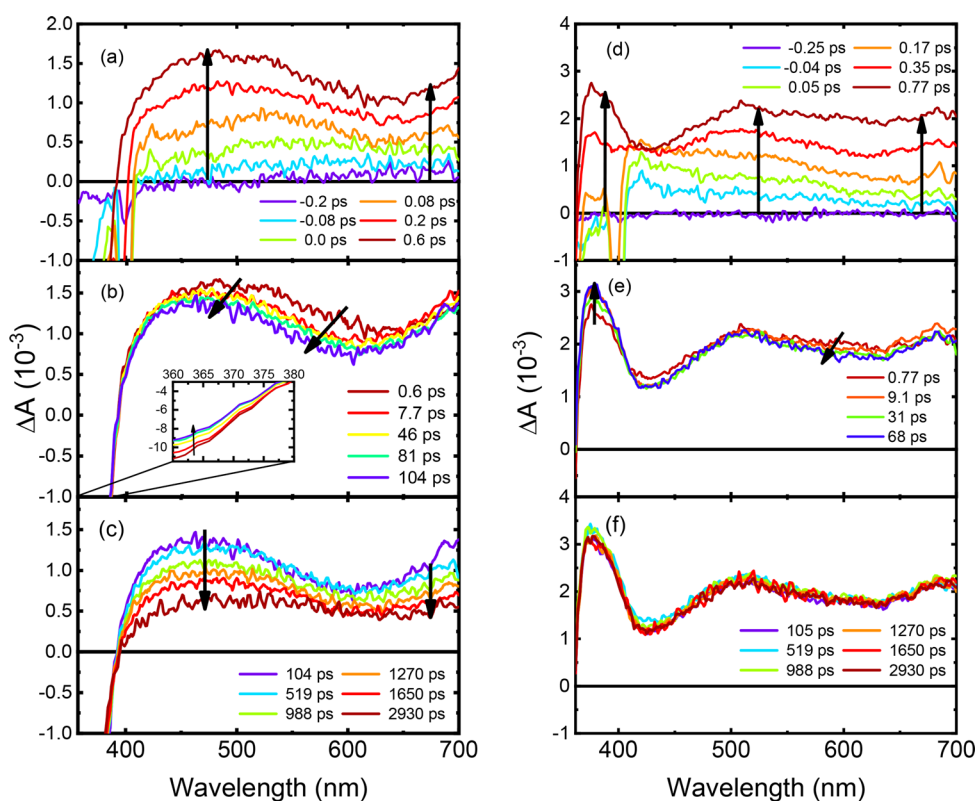


**Figure 2.** (a–c) TAS for 6SeGua following 352 nm excitation through a time delay of 3 ns. (b, inset) Ground-state recovery concurrent with blue-shift of the 490 nm band. (d–f) TAS for 6tGua obtained back-to-back with 6SeGua. The stimulated Raman emission band of water is observed around 400 nm within the cross correlation of the pump and probe beams. TAS were obtained in pH 7.4 PBS at room temperature under  $N_2$ -purged conditions (see SI for details).

to characterize the excited states available to UVA excitation. A complete summary of computational results is given in Tables S1 to S3 and Figure S2. UVA excitation of 6SeGua in aqueous solution excites the  $S_2(\pi\pi^*)$  state. Four lower-lying states are also available for electronic relaxation, namely, a dark  $S_1(n\pi^*)$  state and three triplet states. Both the  $S_2(\pi\pi^*)$  and  $T_3(\pi\pi^*)$  states, as well as the  $S_1(n\pi^*)$  and  $T_2(n\pi^*)$  states, are isoenergetic within computational uncertainty. The  $S_1(n\pi^*)$  and  $T_1(\pi\pi^*)$  states are separated by an energy gap of 0.64 eV.

Femtosecond broadband transient absorption experiments were performed to unveil the electronic decay pathways following UVA excitation. The dynamics of selenium

substitution at the  $C^6$  position were compared to sulfur substitution by performing successive experiments on both 6SeGua and 6tGua. Figure 2 shows the transient absorption spectra (TAS) of 6SeGua and 6tGua following 352 nm excitation. For 6SeGua, two bands appear concurrently on a sub-picosecond time scale: one with a maximum of ca. 490 nm and another with a tail apparent at 675 nm. A negative amplitude signal is observed at short wavelengths immediately after excitation. The signal overlaps with the ground-state absorption spectrum in Figure 1 and is assigned to ground-state depopulation. From a delay time of 0.6 to 104 ps, the 490 nm band blue-shifts 30 nm. Simultaneous to this shift, the

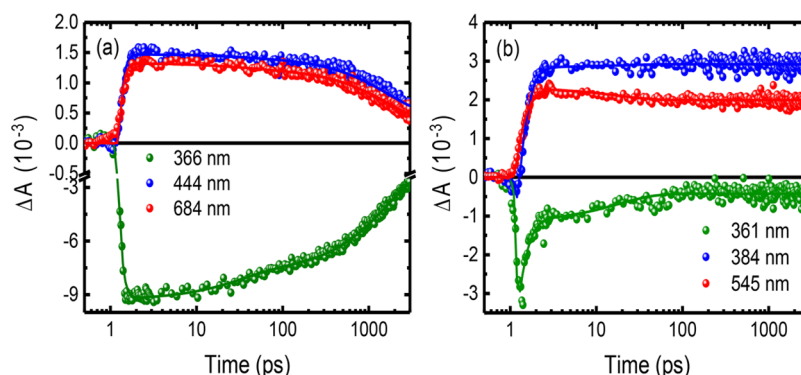


**Figure 3.** Kinetics decay traces for (a) 6SeGua and (b) 6tGua, featuring global fits yielded by a sum of exponentials model.

ground-state recovery signal increases in amplitude (Figure 2b, inset). Following the blue-shift, all spectral features decay uniformly through 3 ns.

The TAS for 6tGua (Figure 2d–f) are similar to those of 6SeGua and consistent with those reported by Ashwood et al.<sup>22</sup> A UV band at ca. 375 nm, a visible band at ca. 500 nm, and a ground-state depopulation signal are observed on a sub-picosecond time scale. The UV band increases in amplitude from a time delay of 0.77 to 68 ps, while the red edge of the visible band narrows. Like 6SeGua, a slight increase in negative amplitude signal occurs during this process. No apparent spectral changes occur from 68 ps through 3 ns.

Kinetics traces corresponding to the TAS in Figure 2 were analyzed globally. Figure 3 shows representative traces with fits obtained from three- and two-lifetime sums of exponential functions for 6SeGua and 6tGua, respectively. Lifetimes obtained from these fits are reported in Table 1. For both

**Table 1. Global Lifetimes for 6SeGua and 6tGua Following Excitation at 352 nm under N<sub>2</sub>-Saturated Conditions**

	lifetime		
	$\tau_1$ /ps	$\tau_2$ /ps	$\tau_3$ /ns
6SeGua	$0.13 \pm 0.05$	$31 \pm 2$	$1.7 \pm 0.1^a$
6tGua	$0.35 \pm 0.04^b$	$18 \pm 1$	$1420 \pm 180^c$

<sup>a</sup>Estimated by extrapolating fit past 1 ns. <sup>b</sup>Same lifetime value was obtained within experimental uncertainties exciting at 342 nm. <sup>c</sup>Reproduced from ref 22, where an excitation wavelength of 345 nm was used.

6SeGua and 6tGua,  $\tau_1$  reflects ultrafast ISC responsible for growth of the  $T_1(\pi\pi^*)$  absorption bands,  $\tau_2$  corresponds to spectral evolution shown in Figure 2b, and  $\tau_3$  corresponds to the uniform triplet decay.

The TAS for 6SeGua and 6tGua are qualitatively similar through the second lifetime. Concurrent to ground-state depopulation, the 490 and 675 nm bands rise during  $\tau_1$ . We assign the rise of these two bands to  $T_1(\pi\pi^*)$  absorption. This assignment is supported by the fact that 6tGua undergoes an ultrafast ISC event following UVA excitation and similarly shows  $T_1(\pi\pi^*)$  absorption with maxima at 375 and 500 nm.<sup>22</sup> Heavy atom substitution enhances ISC dynamics in 6tGua relative to guanine,<sup>22</sup> and selenium substitution should further enhance ISC relative to 6tGua. Indeed, the spin–orbit coupling between the  $S_1(n\pi^*)$  and  $T_1(\pi\pi^*)$  states increases nearly 5-fold for 6-selenoguanosine compared to 6-thioguanosine.<sup>21</sup> 6SeGua's ISC lifetime ( $\tau_1$ ), which is 3 times faster than that in 6tGua, may increase the triplet yield (assuming that the

lifetime of any other competitive relaxation pathway is similar in both molecules), arguably rendering 6SeGua a more effective photosensitizer when incorporated in DNA/RNA.

El-Sayed's propensity rules suggest that ultrafast ISC should occur between singlet and triplet states of different character.<sup>27,28</sup> Pathways that obey this rule for 6SeGua include  $S_2(\pi\pi^*) \rightarrow T_2(n\pi^*)$  and  $S_1(n\pi^*) \rightarrow T_1(\pi\pi^*)$  (Figure S2). Calculations for 6-selenoguanosine and 6-thioguanosine predict that ISC predominately occurs via the  $S_1(n\pi^*) \rightarrow T_1(\pi\pi^*)$  pathway.<sup>21</sup> However, nonadiabatic dynamics simulations indicate that ISC in 6tGua predominately occurs from the  $S_1(n\pi^*)$  minimum to the  $T_2(n\pi^*)$  state.<sup>29</sup> Given the similarities between the theoretical and experimental results for 6SeGua and 6tGua in this study, the  $S_1(n\pi^*) \rightarrow T_2(n\pi^*)$  ISC pathway cannot be excluded. Collectively, the theoretical results suggest that after excitation of 6SeGua to the  $S_2(\pi\pi^*)$  state electron population internally converts to the  $S_1(n\pi^*)$  state before ISC to the  $T_2(n\pi^*)$  and/or  $T_1(\pi\pi^*)$  state occurs:  $S_2 \rightarrow S_1 \rightarrow T_2 \rightarrow T_1$ .

The spectral dynamics that occur during  $\tau_2$  are also similar for both 6SeGua and 6tGua. The blue-shift of the 495 nm band to 460 nm in 6SeGua and the narrowing of the visible band in 6tGua both suggest vibrational relaxation during  $\tau_2$ . Thus, the blue-shift is assigned to vibrational cooling of the hot  $T_1(\pi\pi^*)$  state following population via ultrafast ISC (see Figures S2 and S3). This assignment is supported by the observation that the shifting process is completed prior to the uniform decay of both triplet bands, and excess vibrational energy is dissipated prior to the monotonic decay of the  $T_1(\pi\pi^*)$  state.<sup>30,31</sup>

The negative amplitude signal at ca. 370 nm increases simultaneously to vibrational cooling of the  $T_1(\pi\pi^*)$  state. This phenomenon is also observed for 6tGua,<sup>22</sup> for which it was unclear whether the increase was due to ground-state recovery or overlap with a growing UV band (Figure 2e). For 6SeGua, this event corresponds to ground-state recovery, as the absorption change at 360 nm (ca. 2 mΔA) is an order of magnitude larger than the decline of the 495 nm band (ca. 0.2 mΔA). This event is therefore concurrent, yet unrelated to the vibrational cooling dynamics observed in the  $T_1(\pi\pi^*)$  state. Ground-state recovery during  $\tau_2$  may be achieved via internal conversion of a residual  $S_1(n\pi^*)$  state population to the ground state. Triplet self quenching is an unlikely mechanism,<sup>11,32,33</sup> as it was not supported by preliminary experiments in which the relative absorbance of the 6SeGua solution or pump excitation intensity was varied by 60 to 68%, respectively.

The most remarkable difference between 6SeGua and 6tGua is manifested in  $\tau_3$ . Kinetic traces for 6tGua reach an offset following  $\tau_2$ , indicating that further relaxation events occur on a nanosecond time scale. Previous work has shown that triplet decay occurs over 1420 ns under  $N_2$ -saturated conditions.<sup>22</sup> Due to its long-lived triplet state, photoexcited 6tGua sensitizes singlet oxygen with a 21% yield.<sup>22</sup> 6SeGua instead exhibits immediate, uniform decay of both triplet bands following  $\tau_2$ . Simultaneous recovery of the ground-state bleaching signal confirms that this event represents triplet decay with a lifetime of 1.7 ns (Figure 3). In addition to the stronger  $T_1/S_0$  spin-orbit coupling in 6SeGua than in 6tGua, we argue that there is a smaller energy barrier to access the region of the  $T_1$  potential energy surface where the ISC event occurs, explaining the 835-fold faster triplet decay in 6SeGua.<sup>34</sup> Given the sub-2 ns triplet decay lifetime, the yield of singlet oxygen generation for 6SeGua should be smaller than for 6tGua because diffusional encounter to sensitize molecular oxygen becomes less competitive as the rate of triplet decay increases.

The incorporation of 6SeGua into DNA and RNA has been demonstrated,<sup>35–37</sup> and molecular dynamics simulations have shown that 6SeGua-substituted DNA duplexes are stable.<sup>38,39</sup> Hence, regardless of the sub-2 ns triplet decay lifetime, the incorporation of 6SeGua into DNA/RNA duplexes should increase the probability that a reaction between the triplet state of 6SeGua and an adjacent nucleobase may occur. The close contact of 6SeGua to an adjacent  $\pi$ -stacked canonical nucleobase in a DNA/RNA duplex relaxes the requirement of diffusional encounter for a reaction to occur, enabling 6SeGua to photosensitize damage to DNA before triplet-state decay. Indeed, 6SeGua is a known chemotherapeutic agent.<sup>40</sup> The results presented in this study further show that it is prudent to investigate the photosensitization mechanism of 6SeGua-substituted DNA/RNA duplexes prior to studying tellurium-substituted nucleobases. The substitution with tellurium atoms is expected to further increase the rate of triplet decay to the ground state, which may further decrease the probability of a photosensitized reaction with an adjacent nucleobase compared to a selenium-substituted nucleobase.

## ■ ASSOCIATED CONTENT

### 📄 Supporting Information

The Supporting Information is available free of charge on the ACS Publications website at DOI: 10.1021/jacs.8b07665.

Materials and computational and experimental methods; data analysis and supporting results; single-electron transitions and character composition of computed excited states; Kohn–Sham orbitals corresponding to vertical electronic transitions; Jablonski diagrams; plot of depth of tissue penetration; decay-associated spectra obtained from sum of exponential model; procedure for synthesis of 6-selenoguanine; NMR spectra (PDF)

## ■ AUTHOR INFORMATION

### Corresponding Author

\*carlos.crespo@case.edu

### ORCID

Carlos E. Crespo-Hernández: 0000-0002-3594-0890

### Present Addresses

<sup>§</sup>Participated as an undergraduate research assistant. Department of Chemistry, University of Wisconsin–Madison, Madison, Wisconsin 53706, United States.

<sup>¶</sup>Lawrence Berkeley National Laboratory, AMO Experimental Group, Chemical Sciences Division, Berkeley, California 94720, United States.

### Notes

The authors declare no competing financial interest.

## ■ ACKNOWLEDGMENTS

The authors acknowledge funding from the National Science Foundation (Grant No. CHE-1800052). The Faculty Early Career Development Program from NSF (Grant Nos. CHE-1255084 and CHE-1539808) is also acknowledge for initial support of this work. The authors also thank Mr. Sean Hoehn and Mr. Luis Rodríguez-Ortiz for performing preliminary TAS experiments for 6SeGua at different excitation intensities and concentrations.

## ■ REFERENCES

- (1) Crespo-Hernández, C. E.; Cohen, B.; Hare, P. M.; Kohler, B. *Chem. Rev.* **2004**, *104*, 1977–2019.
- (2) Middleton, C. T.; de La Harpe, K.; Su, C.; Law, Y. K.; Crespo-Hernández, C. E.; Kohler, B. *Annu. Rev. Phys. Chem.* **2009**, *60*, 217–239.
- (3) Improta, R.; Santoro, F.; Organo, C.; Blancafort, L. *Chem. Rev.* **2016**, *116*, 3540–3593.
- (4) Beckstead, A. A.; Zhang, Y.; de Vries, S.; Kohler, B. *Phys. Chem. Chem. Phys.* **2016**, *18*, 24228–24238.
- (5) The International Agency for Research on Cancer. *Monographs on the Evaluation of Carcinogenic Risks to Humans* **2012**, *110D*, 35–101.
- (6) World Health Organization. (2018). *The Known Health Effects of UV* [online]. Available at <http://www.who.int/uv/faq/uvhealthfac/en/> [Accessed July 15, 2018].
- (7) Reichardt, C.; Guo, C.; Crespo-Hernández, C. E. *J. Phys. Chem. B* **2011**, *115*, 3263–3270.
- (8) Taras-Goślińska, K.; Burdziński, G.; Wenska, G. *J. Photochem. Photobiol., A* **2014**, *275*, 89–95.
- (9) Pollum, M.; Jockusch, S.; Crespo-Hernández, C. E. *J. Am. Chem. Soc.* **2014**, *136*, 17930–17933.
- (10) Ashwood, B.; Pollum, M.; Crespo-Hernández, C. E. *Photochem. Photobiol.* **2018**, DOI: 10.1111/php.12975.
- (11) Pollum, M.; Martínez-Fernández, L.; Crespo-Hernández, C. In *Photoinduced Phenomena in Nucleic Acids I, Topics in Current Chemistry*; Springer: Cham, 2015; Vol. 355, pp 245–327.
- (12) Pollum, M.; Lam, M.; Jockusch, S.; Crespo-Hernández, C. E. *ChemMedChem* **2018**, *13*, 1044–1050.
- (13) Pollum, M.; Jockusch, S.; Crespo-Hernández, C. E. *Phys. Chem. Chem. Phys.* **2015**, *17*, 27851–27861.
- (14) Reelfs, O.; Karran, P.; Young, A. R. *Photochem. Photobiol. Sci.* **2012**, *11*, 148–154.
- (15) Pridgeon, S. W.; Heer, R.; Taylor, G. A.; Newell, D. R.; O'Toole, K.; Robinson, M.; Xu, Y.-Z.; Karran, P.; Boddy, A. V. *Br. J. Cancer* **2011**, *104*, 1869–1876.
- (16) Brem, R.; Daehn, I.; Karran, P. *DNA Repair* **2011**, *10*, 869–876.
- (17) Favre, A.; Saintomé, C.; Fourrey, J.; Clivio, P.; Laugâa, P. *J. Photochem. Photobiol., B* **1998**, *42*, 109–124.
- (18) Favre, A. In *Bioorganic Photochemistry*, Volume 1: Photochemistry and the Nucleic Acids; Wiley, 1990; pp 379–425.
- (19) Gemenetzidis, E.; Shavorskaya, O.; Xu, Y.-Z.; Trigiante, G. *J. Dermatol. Treat.* **2013**, *24*, 209–214.
- (20) Pirillo, J.; de Simon, B. C.; Russo, N. *Theor. Chem. Acc.* **2016**, *135*, 1–5.
- (21) Pirillo, J.; Mazzone, G.; Russo, N.; Bertini, L. *J. Chem. Inf. Model.* **2017**, *57*, 234–242.
- (22) Ashwood, B.; Jockusch, S.; Crespo-Hernández, C. E. *Molecules* **2017**, *22*, 379.

- (23) Venkateswarlu, D.; Leszczyński, J. *J. Phys. Chem. A* **1998**, *102*, 6161–6166.
- (24) Leszczyński, J. *J. Mol. Struct.: THEOCHEM* **1994**, *311*, 37–44.
- (25) Karthika, L.; Senthilkumar, R.; Kanakaraju, M. *Struct. Chem.* **2014**, *25*, 197–213.
- (26) Kim, Y.; Jang, Y. H.; Cho, H.; Hwang, S. *Bull. Korean Chem. Soc.* **2010**, *31*, 3013–3016.
- (27) El-Sayed, M. A. *J. Chem. Phys.* **1963**, *38*, 2834–2838.
- (28) El-Sayed, M. A. *J. Chem. Phys.* **1962**, *573*, 573–574.
- (29) Martínez-Fernández, L.; Corral, I.; Granucci, G.; Persico, M. *Chem. Sci.* **2014**, *5*, 1336–1347.
- (30) Kasha, M. *Discuss. Faraday Soc.* **1950**, *9*, 14–19.
- (31) Kasha, M.; McGlynn, S. P. *Annu. Rev. Phys. Chem.* **1956**, *7*, 403–424.
- (32) Reichardt, C.; Crespo-Hernández, C. E. *Chem. Commun.* **2010**, *46*, 5963–5965.
- (33) Reichardt, C.; Crespo-Hernández, C. E. *J. Phys. Chem. Lett.* **2010**, *1*, 2239–2243.
- (34) It is possible that the presence of a deprotonated anionic species of 6SeGua in equilibrium with the neutral form<sup>26</sup> at pH 7.4 may contribute to the observed dynamics. Additional experiments in which the pH of the solution is systematically varied are necessary in order to examine the putative extent of participation of deprotonated species in the dynamics under physiological conditions. Such an investigation is currently underway in our group, but outside of the scope of the present communication.
- (35) Salon, J.; Gan, J.; Abdur, R.; Liu, H.; Huang, Z. *Org. Lett.* **2013**, *15*, 3934–3937.
- (36) Salon, J.; Jiang, J.; Sheng, J.; Gerlits, O. O.; Huang, Z. *Nucleic Acids Res.* **2008**, *36*, 7009–7018.
- (37) Kuar, M.; Rob, A.; Caton-Williams, J.; Huang, Z. *ACS Symp. Ser.* **2013**, *1152*, 89–126.
- (38) Salon, J.; Sheng, J.; Jiang, J.; Chen, G.; Caton-Williams, J.; Huang, Z. *J. Am. Chem. Soc.* **2007**, *129*, 4862–4863.
- (39) Faustino, I.; Curutchet, C.; Luque, F. J.; Orozco, M. *Phys. Chem. Chem. Phys.* **2014**, *16*, 1101–1110.
- (40) Ross, A. F.; Agarwal, K. C.; Chu, S. H.; Parks, R. E. *Biochem. Pharmacol.* **1973**, *22*, 141–154.